



Research Paper

Design a Graphene Based Plasmonic Switch on Flexible Substrate for Terahertz Optical Transmission

Saurav Kumar*, PriyavandBundela, Pradeep Kumar Khiriya, Gagan Kant Tripathi, Purnima SwarupKhare

School of Nanotechnology, Rajiv Gandhi ProudyogikiVishwavidyalaya, Bhopal, Madhya Pradesh,

ABSTRACT: Graphene is a thin, light, flexible, mechanically strong material that is also optically transparent, electrically tunable, and extremely conductive when doped, because graphene has intrinsic plasmons that are programmable and adjustable, it opens up a world of possibilities for traditional plasmonics. Plasmonics provides an appealing solution to electronics' restrictions, which confine electromagnetic waves to the metal-dielectric interface. The finite element analysis approach is used to investigate a graphene-based plasmonic waveguide on a flexible medium in this research. The waveguide is made out of graphene embedded in a polymer cladding that is UV curable and made of fluorinated acrylate polymer (ZPU12). Surface plasmonpolariton waves can be contained and propagated with negligible bending and radiation losses on curved Graphene surfaces embedded in ZPU12. This paper also investigates the properties of surface plasmonpolariton using mathematical computation. In addition, the influence of cladding material on the performance of graphene based plasmonic waveguide is investigated, using two different medium, air and ZPU12 are cross compared.

KEYWORDS: Graphene, Surface PlasmonsPlariton, ZPU12, Plasmonics, Terahertz Optical Transmission

Received 08 November, 2021; Revised: 22 November, 2021; Accepted 24 November, 2021 © The author(s) 2021. Published with open access at www.questjournals.org

I. INTRODUCTION

Graphene has become a subject of intense interest in the research community due to its unique properties [1]. Remarkable efforts have been made on the analysis on both electronic and optical properties. Graphene is a one-atom-thick two dimensional system with extraordinary optical and electrical properties that can be utilized in many potential applications [2, 3]. The outstanding property of graphene comes from its unique crystal structure. Additionally, graphene offers the advantage of tuneable surface plasmons at specific THz frequencies [4]. These features provide applications for the design of a variety of graphene-based optical waveguides, which have been demonstrated experimentally and theoretically [5]. Surface plasmons can propagate in the terahertz and infrared frequency bands because of their unique electric properties, which can be regulated by simply introducing an external magnetostatic or electrostatic field [6-8]. Surface Plasmons Polaritons (SPPs) on graphene have a number of benefits over traditional materials like silver or gold, including tunability, minimal losses, and extreme mode confinement [9, 10]. Several research publications have investigated the features of plasmons propagating over 2D graphene sheets and ribbons/strips and various configurations to improve their guiding qualities have already been presented [11, 12]. The capability to permit or prevent SPP propagation on these structures is a critical component of future plasmonic devices.

Several works have been reported about the propagation of surface plasmon modes excited on different structures of graphene. Coupling of dipole emitter excitement at a varying frequency ranges from 10s of THz to few 100s of THz, which have been examined on different structures of graphene including film, nanoribbon and nanodisk. Koppens et al [13] showed the existence of surface plasmon with high energy and confinement for highly doped graphene. The generation of waveguide and edge modes was studied on graphene micro-ribbons as well as on an array of periodic graphene ribbons as a function of variation in the micro-ribbon width. It was demonstrated that the number of surface plasmon modes on graphene micro-ribbon increase with frequency as well as the width of the ribbon [14].

In this work, the properties of SPP waves on flexible graphene waveguide using ZPU 12 as dielectric medium were investigated. Plasmonic waveguides utilizing the features of low dimensional evanescent waves

*Corresponding Author:Saurav Kumar17 | Page

School of Nanotechnology, Rajiv Gandhi ProudyogikiVishwavidyalaya, Bhopal, Madhya Pradesh

provide the opportunity to confine light to sub-wavelength dimension. Graphene based plasmonic waveguide on flexible dielectric material (ZPU 12) explored using the finite element analysis. Their SPP characteristics have been cross-compared for different chemical doping of graphene.

II. SIMULATION METHODOLOGY

COMSOL Multiphysics is finite element analysis solver and simulation software for various physics and engineering applications. Graphene plasmonic devices can be design by 2D full-wave simulation as follows using RF interface of COMSOL Multiphysics. However, since graphene is a 2D material, graphene parameters including surface conductivity and SPP wave vector cannot use directly into the software. Instead, a special technique to model graphene in 2D simulation software environment is used, which was first introduced by Vakil and Engheta[15, 16].

III. RESULTS & DISCUSSION

A. Strong confinement of SPP waves on graphene

The propagation of SPPs on graphene is strongly dependent on the chemical potential. It has been shown that, for a sufficiently high Fermi level which can be achieved by increasing the chemical potential, the plasmon losses in graphene are very small [17]. Figure 1 shows permittivity of graphene varies as function of frequency. Parameters of free standing graphene, $T = 300$ K, $\Delta=1$ nm, $\Gamma = 3.3$ meV are used. For lower chemical potential ($\mu_c = 0.246$ eV), the real part of equivalent permittivity of graphene remains negative in the working frequency of SPP wave ranges from 20 to 80 THz .However, the frequency ranges from 20 to 250 THz in case of higher chemical potential($\mu_c = 0.8$ eV). Thus, with increase in chemical potential, SPP frequency range can be dramatically expand.

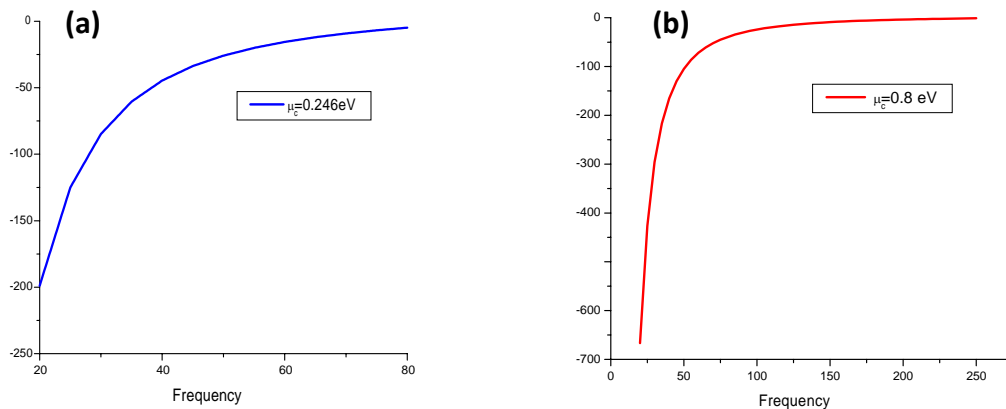


Figure 1:The real parts of equivalent permittivity for free standing graphene as function of input frequency. (a) $\mu_c = 0.246$ eV, and (b) $\mu_c = 0.8$ eV .

Figure 2 shows the propagation length of SPP waves on free-standing graphene normalized by SPP wavelength. Parameters of free standing graphene, $T = 300$ K, $\Delta=1$ nm, $\Gamma = 3.3$ meV are used. The propagation length of SPP wave on graphene with higher chemical potential ($\mu_c = 0.8$ eV) can reach dozens of wavelength compare to lower chemical potential ($\mu_c = 0.2$ eV). Therefore graphene with higher chemical potential is more appropriate in case of propagation length.

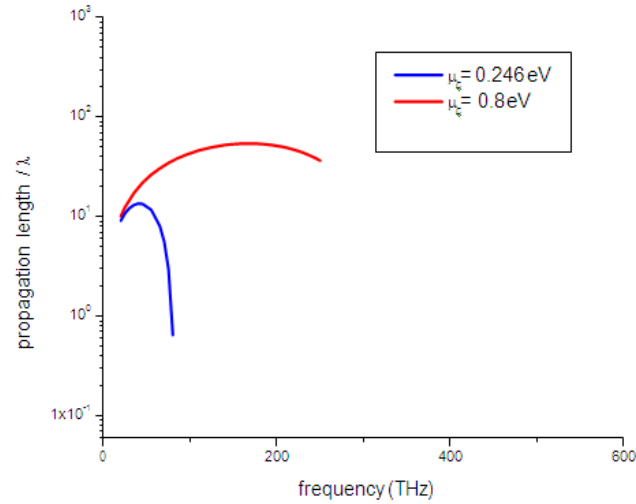


Figure 2: The ratio of propagation length to the SPP wavelength for free standing graphene. (a) $\mu_c = 0.246$ eV, and (b) $\mu_c = 0.8$ eV.

The lateral decay length of SPP waves on free-standing graphene shown in Figure 3. Parameters of free standing graphene, $T = 300$ K, $\Delta = 1$ nm, $\Gamma = 3.3$ meV are used. The SPP waves on graphene have very strong confinements.

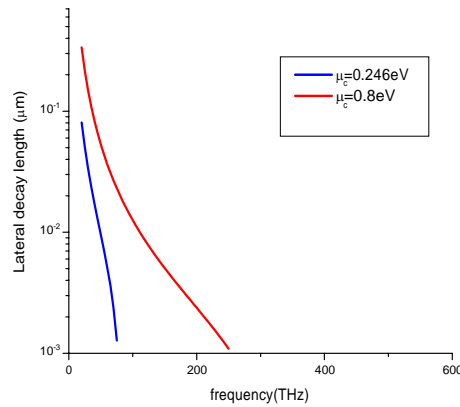


Figure 3: lateral decay length of free standing graphene. (a) $\mu_c = 0.246$ eV, and (b) $\mu_c = 0.8$ eV

In addition, the SPP wave on graphene with lower chemical potential ($\mu_c = 0.2$ eV) has the best confinement, with lateral decay length one or two orders better than that on the graphene surface with higher chemical potential ($\mu_c = 0.8$ eV). Therefore graphene with lower chemical potential is more appropriate in case of confinement. All these simulated results shows good agreement with reference literature [18] indicates graphene material defined properly.

B. SPP waves on free standing graphene surfaces

Figure 4 shows propagation of electric field E_y of SPP waves propagating on straight free standing graphene without any damping. The parameter of graphene, $\Delta = 1$ nm, $\Gamma = 3.3$ meV, $f = 160$ THz and $\mu_c = 0.8$ eV are used.

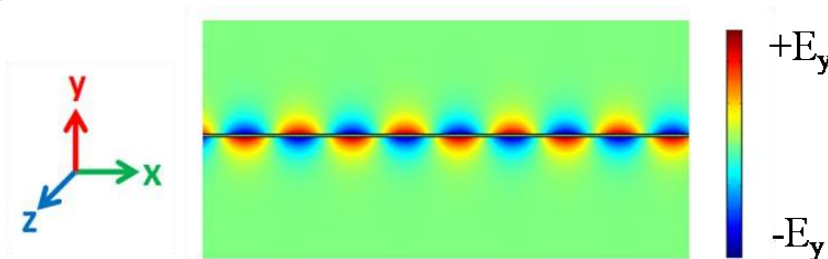


Figure 4: SPP waves on straight free standing graphene surfaces.

C. SPP waves on curved free standing graphene surfaces

The curvature-induced radiative energy loss will affect the SPP propagation efficiencies and the attenuation of SPP wavenumber(k_{spp}), a parameter closely related to the confinement of SPPs. Parameters of free standing graphene, $T = 300$ K, $\Delta=1$ nm, $\Gamma = 3.3$ meV, $f = 160$ THz, and $\mu_c= 0.8$ eV, are used. Scattering loss or the propagation efficiency is estimated by the distribution of tangent magnetic fields along the bending area.

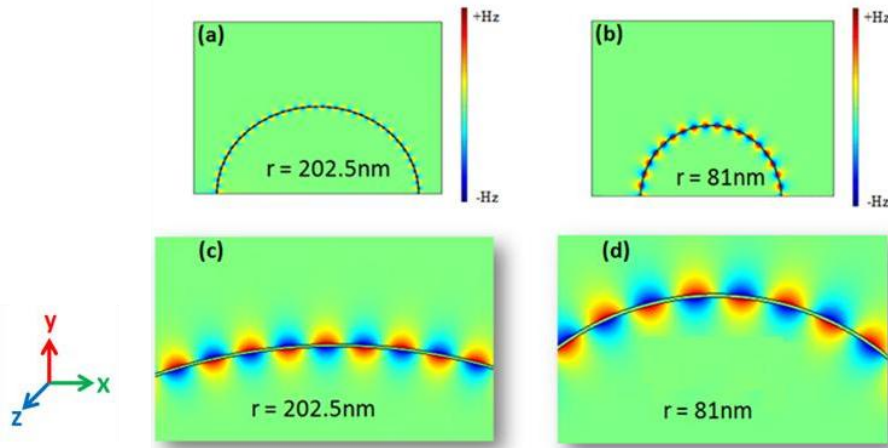


Figure 5: SPP waves on curved free standing graphene surfaces. (c) and (d) are zoomed image of (a) and (b) respectively. (a) , (c) curvature radii is 202.5 nm. (b),(d) radii is 81 nm.

Figure 5 shows, the SPP waves propagate efficiently on the air-graphene-air interfaces with different radii. However, the confinement of SPP waves is decreasing for lower bending radius.

D. SPP properties of graphene embedded in ZPU12 dielectric

Figure 6 shows propagation of electric field E_y of SPP waves propagating on straight graphene embedded in ZPU12 dielectric without any damping. The parameter of graphene, $f=150$ THz, $\Delta=1$ nm, $\Gamma = 3.3$ meV, and $\mu_c= 0.8$ eV are used. Compare to Air, better confinement of SPP waves is achieved in case of ZPU 12.

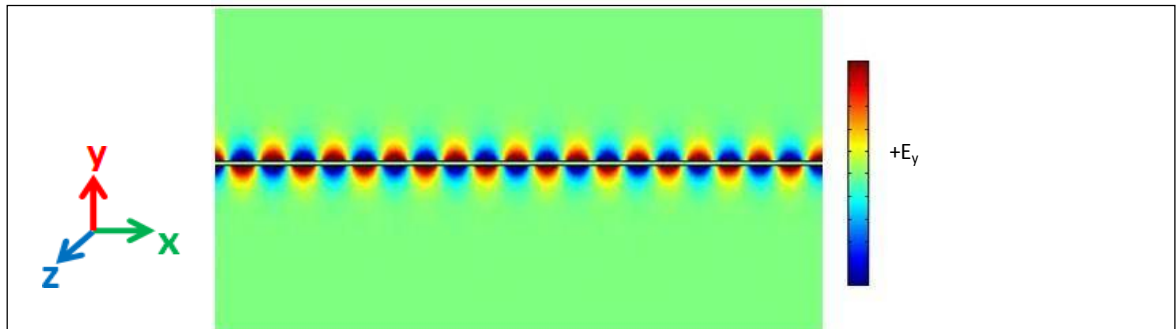


Figure 6:SPP waves on straight graphene waveguide using ZPU 12 as dielectric.

Figure 7 shows dispersion curve for lower chemical potential ($\mu_c= 0.2$ eV) and higher chemical potential ($\mu_c= 0.8$ eV), when graphene surrounded by ZPU12 and Air as dielectric.

Figure 8 shows propagation length as function of frequency, when graphene surrounded by ZPU12 and Air as dielectric. The propagation length increases, with increase in chemical potential. In addition, Air gives higher propagation length compared to ZPU12.

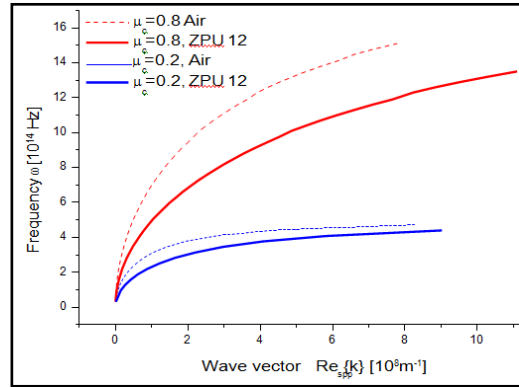


Figure 7: The Dispersion curve for the graphene embedded in ZPU12 (solid line) and Air (dashed line). $\mu_c = 0.2$ eV (blue). $\mu_c = 0.8$ eV (red).

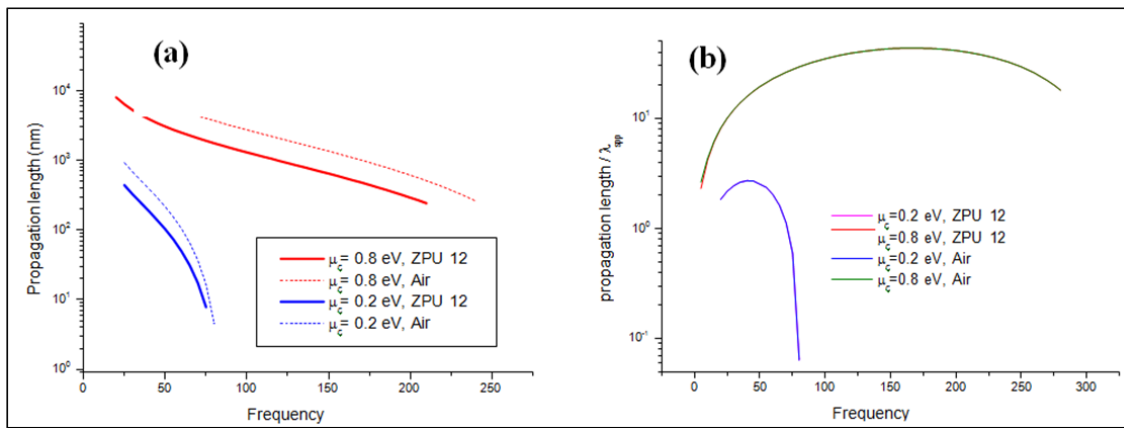


Figure 8: Comparison of the SPP properties on graphene, (a) the propagation length for the graphene embedded in ZPU12 (solid line) and Air (dashed line). $\mu_c = 0.2$ eV (blue). $\mu_c = 0.8$ eV (red). (b) The ratio of propagation length to SPP wavelength for the graphene embedded in ZPU12 and Air. $\mu_c = 0.2$ eV (pink) and $\mu_c = 0.8$ eV (red), when ZPU12 is used as dielectric. $\mu_c = 0.2$ eV (blue) and $\mu_c = 0.8$ eV (green), when Air is used as dielectric.

Figure 9 shows, when propagation length is normalized by SPP wavelength, the normalized propagation length for ZPU12 is same as that of Air, since output frequency is higher in case of ZPU12 compare to Air. Figure 10 also shows lateral decay length as function of frequency, when graphene surrounded by ZPU12 and Air as dielectric. The lateral decay length decreases, with decrease in chemical potential. In addition, ZPU12 gives lower decay length compared to Air. Thus ZPU12 will give higher confinement of SPP waves.

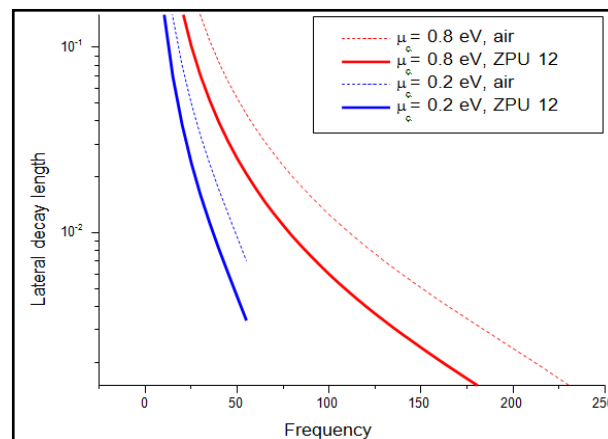


Figure 9: The lateral decay length for the graphene embedded in ZPU12 (solid line) and Air (dashed line). $\mu_c = 0.2$ eV (blue). $\mu_c = 0.8$ eV (red).

Figure 10 shows power as function of input frequency, for both Air and ZPU12 as dielectric. Results shows maximum peak of output power is higher in case of ZPU12 compare to Air. Also, maximum peak of output power occur at lower resonant frequency in case of ZPU12 compare to Air. Figure 13 shows that power is increasing as chemical potential of graphene is increasing.

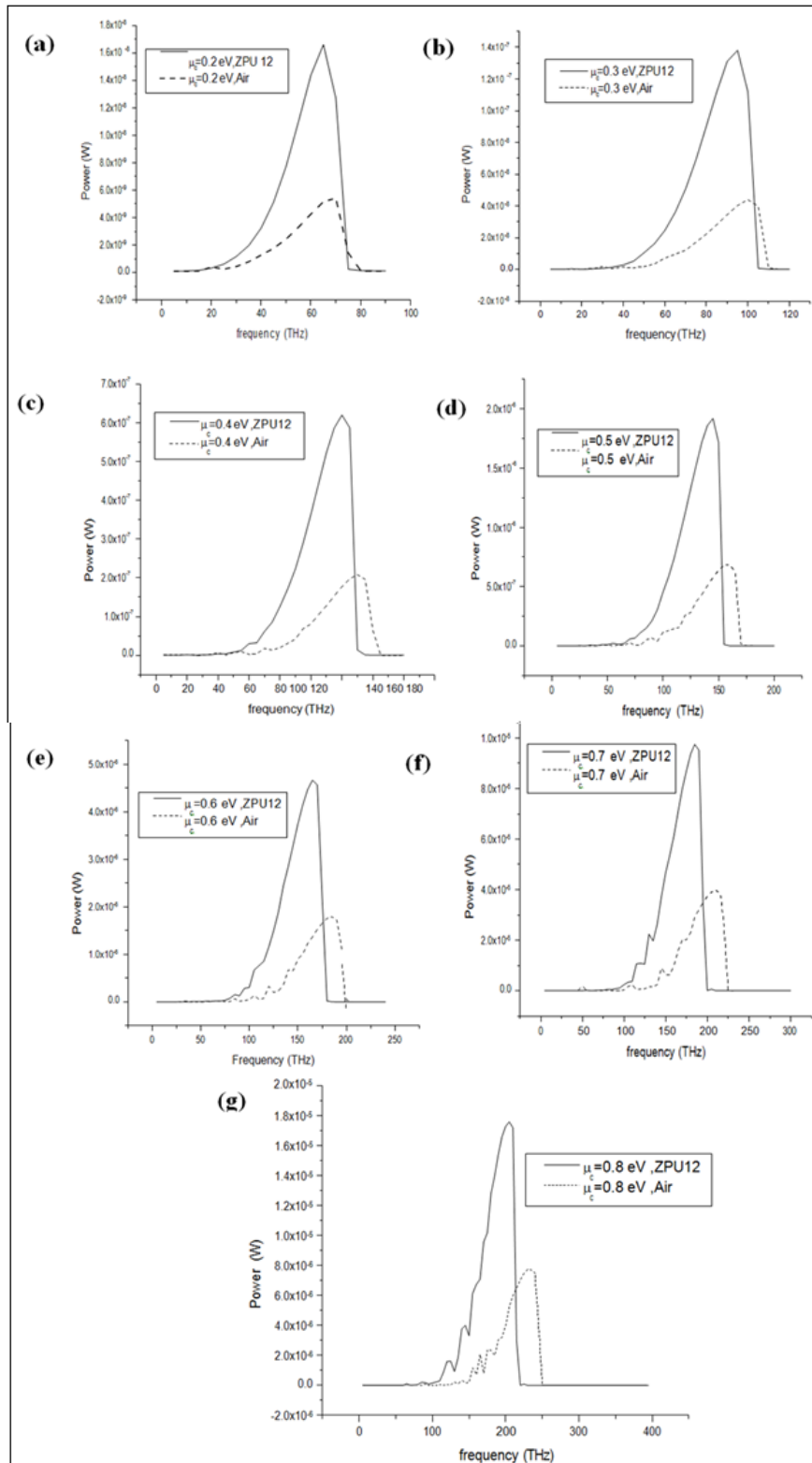


Figure 11: The Power versus frequency plot for the graphene embedded in ZPU12 (solid line) and Air (dashed line). (a), (b), (c), (d), (e), (f), and (g) represents $\mu_c = 0.2$ eV, $\mu_c = 0.3$ eV, $\mu_c = 0.4$ eV, $\mu_c = 0.5$ eV, $\mu_c = 0.6$ eV, $\mu_c = 0.7$ eV, and $\mu_c = 0.8$ eV respectively.

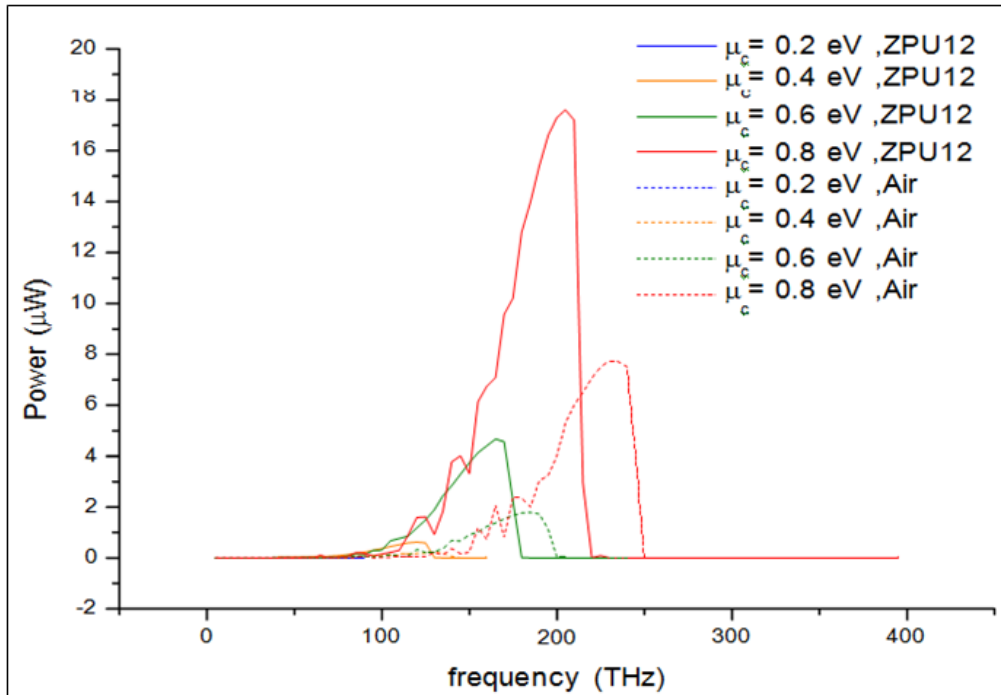


Figure 12: The Power versus frequency plot for the graphene embedded in ZPU12 (solid line) and Air (dashed line). $\mu_c = 0.2$ eV (blue), $\mu_c = 0.4$ eV (orange), $\mu_c = 0.6$ eV (green), and $\mu_c = 0.8$ eV (red).

E. Study of Graphene SPP in bending waveguides with ZPU12 dielectric

Figure 13 shows propagation of tangential magnetic field of SPP waves propagating on curved graphene embedded in ZPU12 dielectric without any damping. The Curvature radius of graphene is 202.5 nm. The parameter of graphene, $f = 150$ THz, $\Delta = 1$ nm, $\Gamma = 3.3$ meV, and $\mu_c = 0.8$ eV are used.

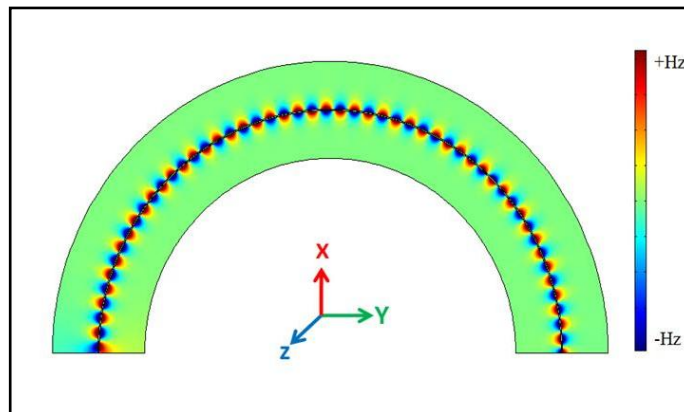


Figure 13: SPP waves on curved graphene layer embedded in ZPU12 dielectric.

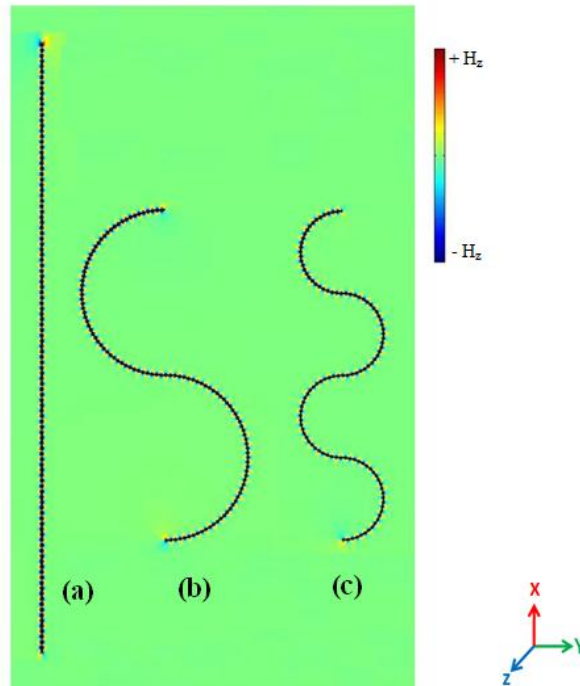


Figure 14: SPP waves on curved graphene layer (length=753.98 nm) embedded in ZPU12 (a) curvature radius= ∞ , (b) curvature radius=119.9 nm, (c) curvature radius= 60 nm.

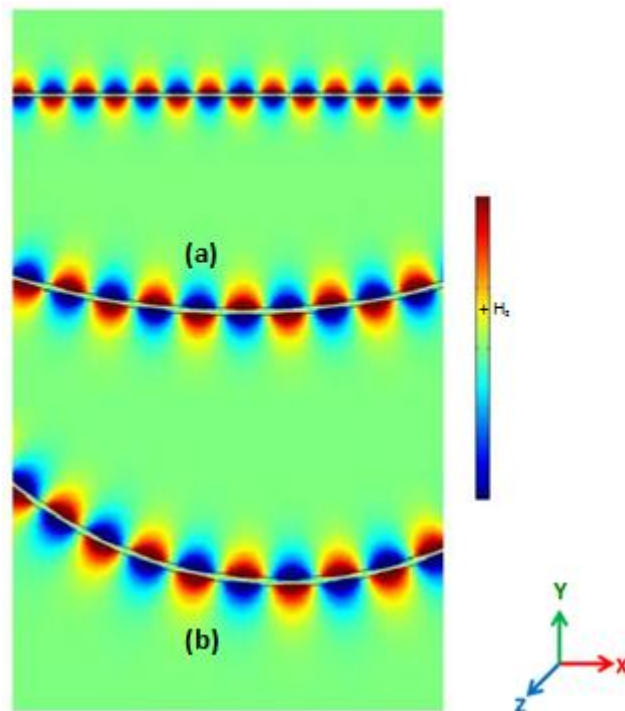


Figure 15: SPP waves on curved graphene layer (length=753.98 nm) embedded in ZPU12 (a) curvature radius= ∞ , (b) curvature radius=119.9 nm, (c) curvature radius= 60 nm.

Figure 14 and Figure 15 shows the propagations of SPP waves on graphene embedded in ZPU12, along arc surfaces with different radii but the same electrical length ($l_{arc}=753.98$ nm). The SPP wave on graphene can propagate through multi bend structure also. However the confinement of SPP waves reduces as bending radius are decreases.

IV. CONCLUSION

In this study, the properties of SPP waves on flexible graphene waveguide using ZPU 12 as dielectric medium were investigated. Plasmonic waveguides utilizing the features of low dimensional evanescent waves provide the opportunity to confine light to sub-wavelength dimension. Graphene based plasmonic waveguide on flexible dielectric material; ZPU 12 is explored using the finite element analysis. Their SPP characteristics have been cross-compared for different chemical doping of graphene. The SPP characteristics of graphene for two different dielectric materials, i.e. Air and ZPU 12 have been cross-compared for different chemical doping of graphene. Compare to Air, ZPU 12 gives higher confinement, higher power in same propagation length. Flexible plasmonic waveguides opens the opportunity to high capacity photonic chips. Since ZPU 12 provides satisfying SPP properties, it can be served as the building block to construct flexible optoelectronic circuits with very small components such as switches, modulators, resonators and couplers. Together with graphene, ZPU 12 can serve as promising dielectric material for flexible plasmonics.

REFERENCES

- [1]. Pendry, J.B., et. al., Mimicking surface plasmons with structured surfaces. *Science*, 2004. 305: p. 847–848.
- [2]. Pitarke, J.M., et. al., Theory of surface plasmons and surface-plasmonpolaritons. *Rep. Prog. Phys.*, 2007. 70: p.1–87.
- [3]. Wang, Y., et. al., Foundations of plasmonics. *Advance Physics*, 2011. 60: p. 799–898.
- [4]. Elser, J., et. al., Plasmonic nanolayer composites: Coupled plasmonpolaritons, effective-medium response, and subdiffraction light manipulation. *Journal. Nanomaterials*, 2007. 79469.
- [5]. Zhao Y., et. al., *Journals of Alloys & Compound*, 2019. 776 31.
- [6]. Dudem B., et. al., *Applied Energy*, 2018. 230 865.
- [7]. Kawata, S., et. al., Plasmonics for near-field nano-imaging and superlensing. *Sensors & Actuators B*, 2009. 3: p.388–394.
- [8]. Homola, J., et. al., Surface plasmon resonance sensors: review. *Sensors & Actuators B*, 1999. 54: p. 3–15.
- [9]. Grigorenko, A.N., et. al., Graphene plasmonics. *Nature Photonics*, 2012. 6: p. 749–758.
- [10]. Koppens, F.H., et. al., Graphene plasmonics: A platform for strong light-matter interactions. *Nano Letters*, 2011. 11: p. 3370–3377.
- [11]. Hanson, G.W., Dyadic green's functions and guided surface waves for a surface conductivity of graphene. *Journal of Applied Physics*, 2008. 103: 064302.
- [12]. Tassin P., et. al., A comparison of graphene, superconductors and metals as conductors for metamaterials and plasmonics. *Nature Photonics*, 2012. 6: 259.
- [13]. Koppens F H L, et. al., Photodetectors based on graphene, other two-dimensional materials and hybrid systems. *Nature Nanotechnology*, 2014. 9: p. 780-793.
- [14]. Nikitin A.Y., et. al., Edge and waveguide terahertz surface plasmon modes in graphene microribbons. *Physica review B*, 2011. 84: p.161407.
- [15]. Vakil, A., et. al., Transformation optics using graphene. *Science*, 2011 332(6035): p. 1291–1294.
- [16]. Andersen, D.R., et. al., Graphene-based long-wave infrared TM surface plasmon modulator. *Journal of the Optical Society of America B*, 2010. 27(4): p. 818–822.
- [17]. Luo, X., et. al., Plasmons in graphene: Recent progress and applications, *Material Science & Engineering R: Reports*, 2013. 74(11): p. 351-376.
- [18]. Lu, W.B., et. al., Flexible transformation plasmonics using graphene, *Optics expres*, 2013. 21(9): 10475.